Analysis of voids in superdrawn polyoxymethylene fibres

Tamikuni Komatsu, Sachio Enoki and Atsushi Aoshima
Technical Research Laboratory of Asahi Chemical Industry Co. Ltd, 2-1 Samejima, Fuji Sizuoka 416, Japan
(Received 8 April 1991; revised 24 July 1991; accepted 31 July 1991)

Void factors (size and distribution) of polyoxymethylene superdrawn fibres were determined, and their relationship to tensile strength was examined. Microvoids $< \sim 0.3\ \mu m^2$ had little effect on strength, while those $> \sim 1\ \mu m^2$ caused a decrease in tensile strength

(Keywords: void analysis; tensile properties; polyoxymethylene; superdrawn fibre)

INTRODUCTION

Structural defects such as voids, kink bands and flaws have been observed in many superdrawn polymers. Clark *et al.*[1,2] found many voids in superdrawn polyoxymethylene (POM) and polypropylene fibres produced by two-step drawing in heated air. These defects influence tensile properties. For highly oriented ultra high molecular weight polyethylene fibres, Smook *et al.*[3] noted that fractures were produced at surface irregularities, such as kink bands, leading to the formation of cracks with fibrillated fracture surfaces. Nakagawa *et al.*[4,5] reported void ratios to increase with draw ratios for large diameter POM fibres produced by microwave heating/drawing. Recently, we studied the relationships between structures and properties (mechanical, chemical and physical properties) for superdrawn POM fibres free of voids and with voids, and found that the properties were influenced by the number of voids in a fibre[6–8].

A theoretical method based on statistical theory and empirical methods using an electron microscope[9,10], acoustic emission[11,12] and small angle X-ray diffraction[13,14] have been used for the analysis of voids. From these methods, electron microscopy was found to be the best for characterizing voids in fibres. The relationships between void factors (size and distribution) and tensile properties of the superdrawn fibres should be carefully studied.

In this work, void factors of superdrawn POM fibres were determined by image analysis using a scanning electron microscope. The relationships between these factors and tensile properties are discussed.

EXPERIMENTAL

Sample preparation

A tube of outer diameter 6.0 mm and inner diameter 1.8 mm was prepared by the melt extrusion of acetal homopolymer (Tenac 3010, Asahi Chemical Industry Co. Ltd), and continuously two-step drawn in silicone oil. The drawing conditions were as follows: in the first step, the vessel length was 2 m, the feed speeds were 0.5 and 1.0 m min^{-1}, the draw ratio (λ) was 8, the drawing temperature was 155°C and the gauge pressure was 0 kg cm^{-2}; in the second step, the vessel length was 12 m, the drawing temperature was 170°C, the gauge pressure was 0 kg cm^{-2} and the fibre was drawn to ductile fracture (conventional fibres). Drawing was also carried out at a high pressure using the same apparatus and conditions as above except for a gauge pressure of 400 kg cm^{-2} (pressurized fibres). Silicone oil adhering to the drawn fibres was completely removed by fresh freon-113. The details have been given previously[7].

Measurements of draw ratio, tensile strength and density

The draw ratio was determined from the ratio of the sample weight per unit length before and after drawing. The tensile strength (σ') was measured using two stainless reel chucks 160 mm in diameter. The cross-sectional area of a sample for calculating σ' was determined from the sample weight and true density (ρ). The value of σ' is thus based on areas exclusive of voids. The value of ρ was calculated from the crystallinity measured by d.s.c.; ρ was 1.42–1.44 g cm^{-3} in this drawing region. The apparent density (ρ_{app}) was measured using a density medium of aqueous potassium carbonate at 23°C for 30 min according to JIS K 7112 (1980). The details have been given elsewhere[7].

Measurement of void factors

The surface structure was observed by a scanning electron microscope (Hitachi-Seisakusho Co., S-430). The electron voltage was 10 kV and the magnification was 5400. The SEM micrographs thus obtained were analysed by an image analyser (Leitz Co., TAS Plus, version TAS 03-P2-RT) connected to a microcomputer (PC). Images of voids were projected onto the analyser screen. Each image, the dark region in the SEM micrograph, was detected from differences in image contrast and stored. The mask area of the SEM micrograph was 226.345 μm^2. The size, number and distribution of voids were mathematically computed. The distribution was obtained by plotting the relation of number to size, or quantity (number × size) to size.

0032-3861/92/102123-05

RESULTS AND DISCUSSION

Tensile strength and apparent density of conventional fibres

Figure 1 shows the relationships of σ' and ρ_{app} to λ for conventional fibres prepared at a feed speed of 0.5 and 1.0 m min^{-1}. The plot of σ' *versus* λ gave a clear curve having a maximum σ' of 1.6 GPa at $\lambda = 17$ and 1.45 GPa at $\lambda = 14$, decreased a little at $\lambda = 19$ and 16, and remarkably decreased at $\lambda = 21$ and 17, at a feed speed of 0.5 and 1.0 m min^{-1}, respectively. The value of ρ_{app} was 1.42 g cm^{-3} at λ corresponding to maximum σ', linearly decreased over λ and reached 1.34 g cm^{-3}. The decrease in ρ_{app} was due to void generation during drawing. The values for σ' are also related to void generation; this is because, σ' showed a maximum at maximum ρ_{app}, and decreased 7–3% and 21–16% at ρ_{app} = 1.37–1.38 and 1.34 g cm^{-3}, respectively. The void fraction at the maximum and minimum σ' was 3–4 and 5–6%, respectively. This rapid decrease in strength thus cannot be explained only by void fraction.

SEM observation of conventional fibres

Figures 2 and *3* show typical SEM photographs of surfaces of conventional fibres prepared at feed speeds of 0.5 and 1.0 m min^{-1} for image analysis, respectively. Small voids were observed up to the peak of σ', but many oval-shaped voids could be seen over the peak. Void size and quantity became larger with decrease in σ' over the peak, particularly at ρ_{app} = 1.34 g cm^{-3}. This was more conspicuous in the fibres prepared at a feed speed of 1.0 m min^{-1}.

Void factors of conventional fibres

Void number, size and quantity (number × size) for *Figures 2* and *3* were determined by image analysis. *Figures 4* and *5* show the relation of void quantity (number × size) to size. Distributions peaked at a size of ~0.05 μm^2. At maximum σ' and near the peak of σ' (ρ_{app} = 1.42–1.37 g cm^{-3}), the void size was < ~0.3 μm^2 and the quantity was small. At minimum σ' (ρ_{app} = 1.34 g cm^{-3}), voids < ~0.3 μm^2 increased conspicuously and those > ~1.0 μm^2 were also generated. The increase in void fraction at minimum σ' was due primarily to the voids < ~0.3 μm^2, but the increase is ~3% compared with that near the peak of σ' (ρ_{app} = 1.37 g cm^{-3}). These results suggest that the microvoids < ~0.3 μm^2 have little effect on the tensile strength, while those > ~1 μm^2, decrease the strength.

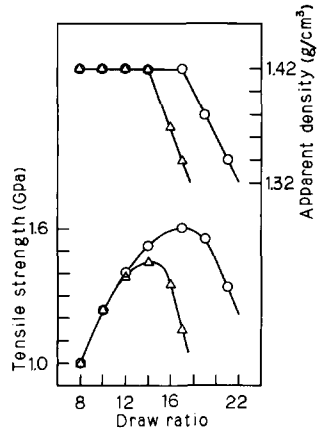

Figure 1 Tensile strength and apparent density *versus* draw ratio for conventional fibres prepared at feed speeds of 0.5 (○) and 1.0 (△) m min^{-1}

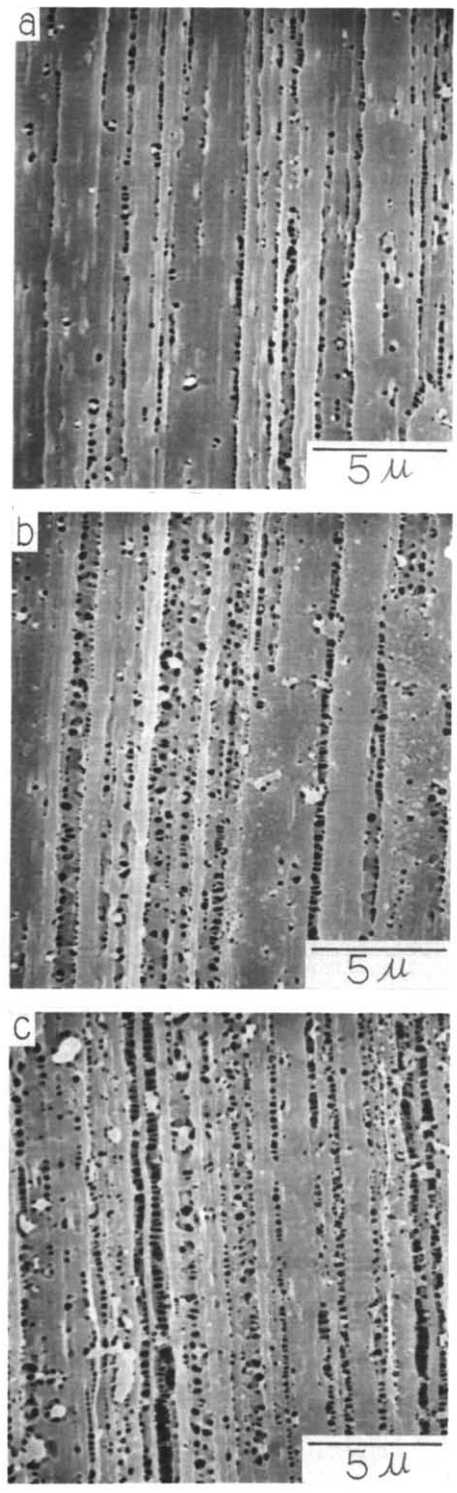

Figure 2 Typical SEM photographs for image analysis of surfaces of conventional fibres prepared at a feed speed of 0.5 m min^{-1}: (a) $\lambda = 17$; (b) $\lambda = 19$; (c) $\lambda = 21$

Tensile strength and apparent density of pressurized fibres

The fibres prepared at high pressure were examined. *Figure 6* shows the relationships of σ' and ρ_{app} to λ for pressurized fibres prepared at feed speeds of 0.5 and 1.0 m min^{-1}. The plots of σ' *versus* λ showed plateau curves. The value of ρ_{app} slowly increased from 1.42 to 1.44 g cm^{-3} and then linearly dropped to 1.31–1.32

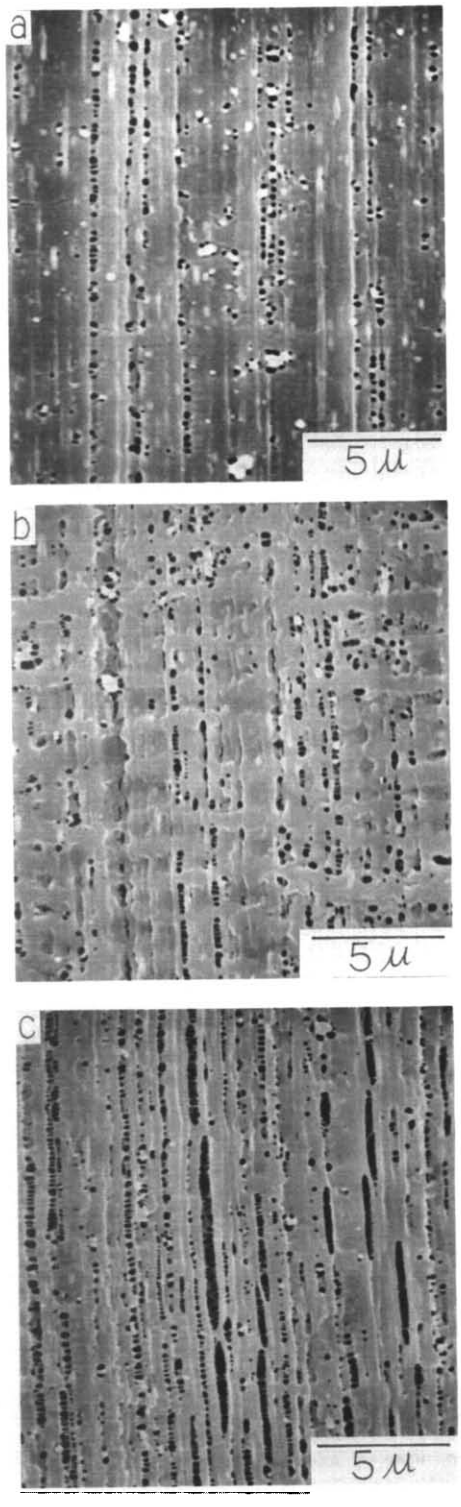

Figure 3 Typical SEM photographs for image analysis of surfaces of conventional fibres prepared at a feed speed of 1.0 m min^{-1}: (a) $\lambda = 14$; (b) $\lambda = 16$; (c) $\lambda = 17$

g cm^{-3}. The value of σ' hardly decreased in spite of the decrease in ρ_{app} over $\lambda = 18$. This indicates that the voids in pressurized fibres exist only as spaces having no influence on strength.

SEM observation of pressurized fibres

Figure 7 and *8* show typical SEM photographs of surfaces of pressurized fibres prepared at feed speeds of 0.5 and 1.0 m min^{-1}, respectively. Macrovoids could hardly be found by SEM, although the existence of voids was clarified for the fibres over $\lambda = 24$ by an equatorial streak scattering in a small angle X-ray scattering photograph besides the remarkable decrease in ρ_{app}. The void size was so small that the void distribution could

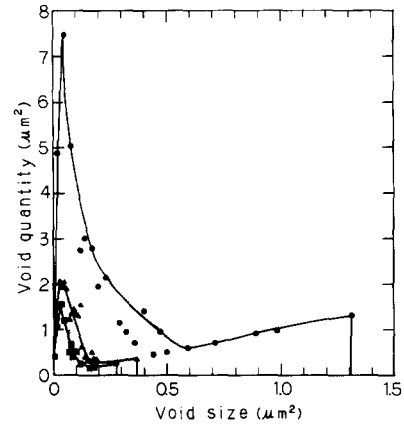

Figure 4 Void quantity (number × size) *versus* size for conventional fibres prepared at a feed speed of 0.5 m min^{-1}: (■) $\lambda = 17$; (▲) $\lambda = 19$; (●) $\lambda = 21$

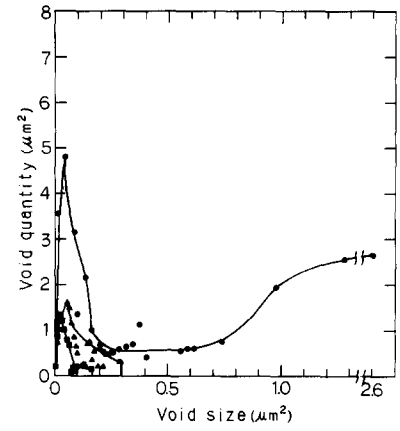

Figure 5 Void quantity (number × size) *versus* size for conventional fibres prepared at a feed speed of 1.0 m min^{-1}: (■) $\lambda = 14$; (▲) $\lambda = 16$; (●) $\lambda = 17$

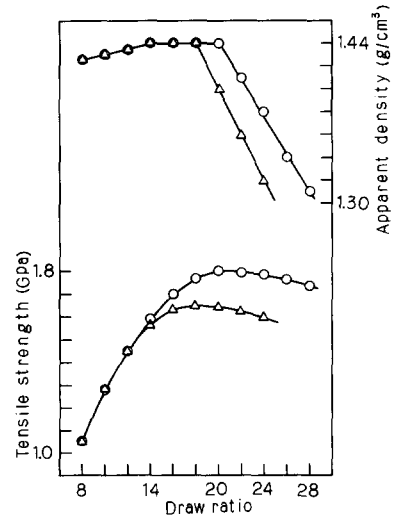

Figure 6 Tensile strength and apparent density *versus* draw ratio for pressurized fibres prepared at feed speeds of 0.5 (○) and 1.0 (△) m min^{-1}

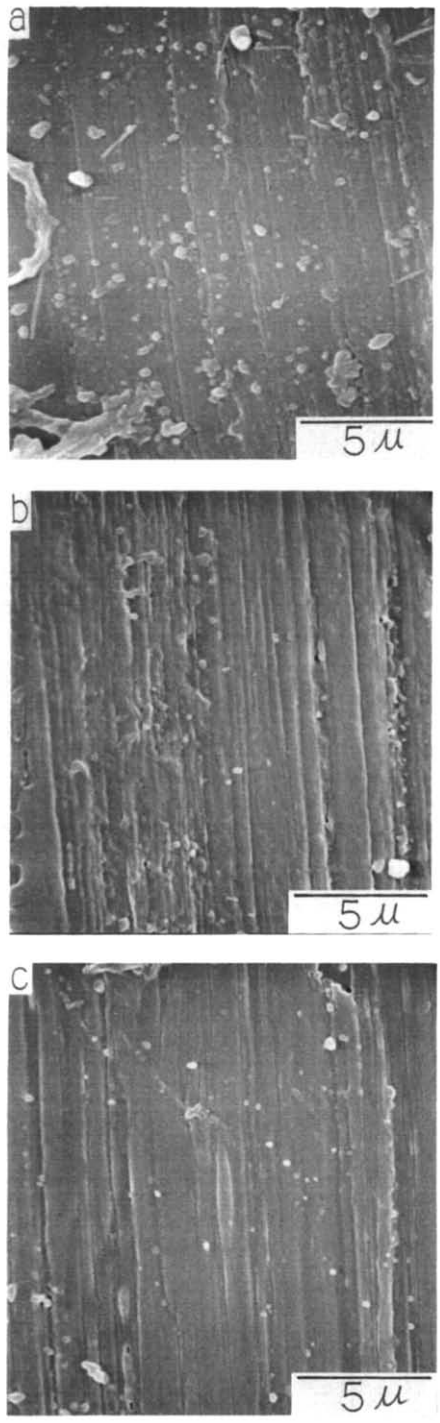

Figure 7 Typical SEM photographs of surfaces of pressurized fibres prepared at a feed speed of 0.5 m min^{-1}: (a) $\lambda = 20$; (b) $\lambda = 22$; (c) $\lambda = 28$

not be measured. Such voids caused no remarkable decrease in strength such as that noted for conventional fibres.

Stress–strain curves of conventional and pressurized fibres

Figure 9 shows typical stress–strain curves for conventional fibres with $\lambda = 17$ and 21 and for pressurized fibres with $\lambda = 18$, 22 and 26 prepared at a feed speed of 0.5 m min^{-1}. Void quantities in the conventional fibres with $\lambda = 17$ and 21 are nearly equal to those in the pressurized fibres with $\lambda = 18$ and 26, respectively. The rupture strain was 8.7% ($\lambda = 17$) and 5.4% ($\lambda = 21$) for conventional fibres, and 8.7% ($\lambda = 18$), 7.1% ($\lambda = 22$) and 5.8% ($\lambda = 26$) for pressurized fibres. The strain generally decreases with increase in λ. The decrease in strain for the conventional fibre with $\lambda = 21$ is much larger than that for the pressurized fibre with $\lambda = 22$. The large decrease in the strain for conventional fibre with $\lambda = 21$ does not arise from only an increase in λ but is also probably related to the stress concentration on macrovoids in the fibre.

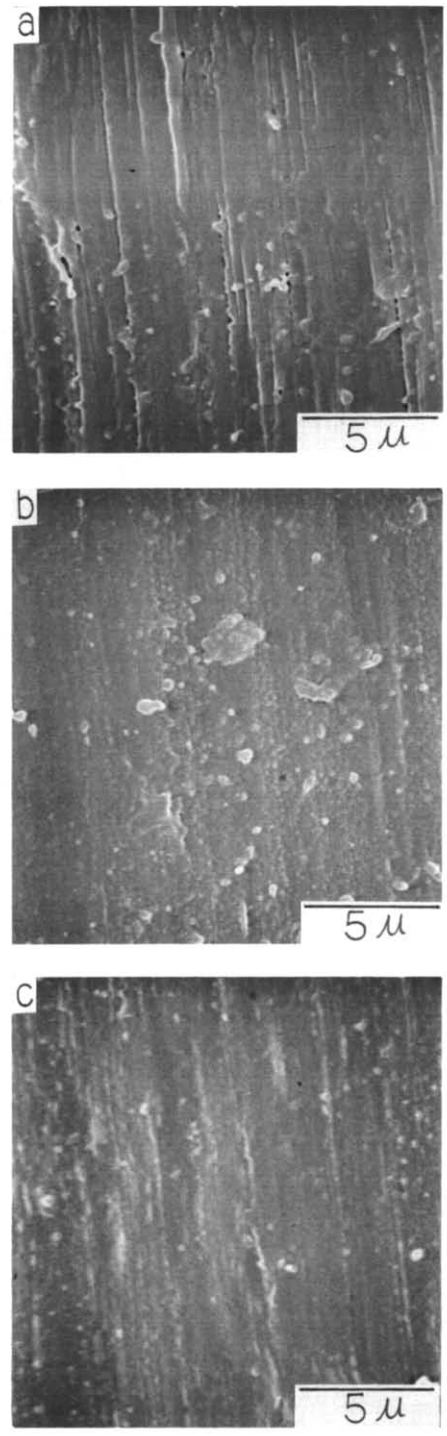

Figure 8 Typical SEM photographs of surfaces of pressurized fibres prepared at a feed speed of 1.0 m min^{-1}: (a) $\lambda = 18$; (b) $\lambda = 20$; (c) $\lambda = 24$

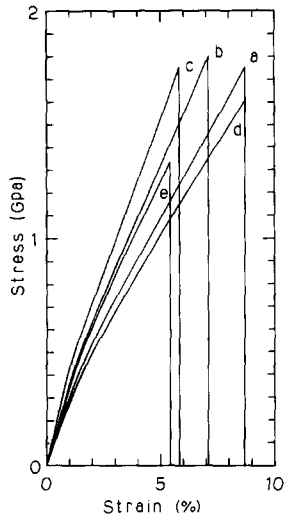

Figure 9 Typical stress–strain curves for conventional and pressurized fibres prepared at a feed speed of 0.5 m min^{-1}: (a) $\lambda = 18(P)$; (b) $\lambda = 22(P)$; (c) $\lambda = 26(P)$; (d) $\lambda = 17(C)$; (e) $\lambda = 21(C)$, where P and C indicate pressurized and conventional fibres, respectively

CONCLUSIONS

Voids of POM superdrawn fibres prepared by the conventional method and pressurized process were analysed. The relationship between void factors (size and distribution) and tensile strength was examined. The void size and quantity of conventional fibres were small at the peak strength. The factors increased beyond this peak with a drop in strength. Microvoids $< \sim 0.3\ \mu m^2$ had little effect on the strength, but beyond $\sim 1\ \mu m^2$ decreased the strength. For fibres prepared at high pressure, the void size was so small that the strength showed virtually no decrease.

REFERENCES

1 Clark, E. S. and Scott, L. S. *Polym. Eng. Sci.* 1974, **14**, 682
2 Taylor, W. N. and Clark, E. S. *Polym. Eng. Sci.* 1978, **18**, 518
3 Smook, J., Hamersma, W. and Pennings, A. J. *J. Mater. Sci.* 1984, **19**, 1359
4 Konaka, T., Nakagawa, K. and Yamakawa, S. *Polymer* 1985, **26**, 462
5 Nakagawa, K. and Konaka, T. *Polymer* 1986, **27**, 1037
6 Komatu, T., Enoki, S. and Aoshima, A. *Polymer* 1991, **32**, 1983
7 Komatu, T., Enoki, S. and Aoshima. A. *Polymer* 1991, **32**, 1988
8 Komatu, T., Enoki, S. and Aoshima, A. *Polymer* 1991, **32**, 1994
9 Kambour, R. P. *J. Polym. Sci., Macromol. Rev.* 1973, **7**, 1
10 Lee, S., Miyaji, H. and Geil, P. H. *J. Macromol. Sci. Phys.* 1983, **B22**, 489
11 Grabec, I. and Peterlin, A. *J. Polym. Sci., Polym. Phys. Edn* 1978, **14**, 651
12 Shichijjo, S., Matsusige, K. and Takemura. T. *Nipponn Leorojii Gakkaishi* 1985, **13**, 70
13 Renninger, A. L. and Uhlmann, D. R. *J. Polym. Sci., Polym. Phys. Edn* 1978, **16**, 2237
14 Wendorff, J. H. *Progr. Colloid Polym. Sci.* 1979, **66**, 135